# Functionalizable Organic Nanochannels Based on Lipid Nanotubes: Encapsulation and Nanofluidic Behavior of Biomacromolecules

Naohiro Kameta,[†] Mitsutoshi Masuda,*[,†,‡] Hiroyuki Minamikawa,[†,‡] Yumiko Mishima,[§] Ichiro Yamashita,[§,||] and Toshimi Shimizu*[,†,‡]

*SORST, Japan Science and Technology Agency, Tsukuba Central 5, 1-1-1 Higashi, Tsukuba, Ibaraki 305-8565, Japan, Nanoarchitectonics Research Center, National Institute of Advanced Industrial Science and Technology, Tsukuba Central 5, 1-1-1 Higashi, Tsukuba, Ibaraki 305-8565, Japan, CREST, Japan Science and Technology Agency, and Graduate School of Material Science, Nara Institute of Science and Technology, 8916-5 Takayama-cho, Ikoma, Nara 630-0192, Japan*

*Received March 6, 2007. Revised Manuscript Received April 24, 2007*

The amino groups on the inner surface of the nanotube that was self-assembled from unsymmetrical bolaamphiphile, *N*-(2-aminoethyl)-*N*′-(β-D-glucopyranosyl)-icosanediamide **1**, were modified covalently with a fluorescence donor dye. This functionalization of the nanotube inner surfaces has allowed us to achieve the construction of an optical recognition system for the encapsulation of guest molecules. Fluorescence resonance energy transfer (FRET) from the fluorescence donor located on the inner surface to the ferritin labeled with fluorescence acceptor enabled us to visualize the encapsulation and nanofluidic features of the ferritin in the nanochannel shaped by the hollow cylinder structure. By using this system, we were able to estimate the diffusion constants for ferritin and gold nanoparticles in the organic nanochannels on the basis of lipid nanotubes. We have also demonstrated that the size and surface charge of the nanochannel strongly affect the encapsulation behavior toward the biomacromolecules such as DNA and spherical proteins.

## Introduction

Supramolecular nanotube architectures self-assembled from amphiphilic molecules have attracted much attention in the field of nanotechnology and biotechnology.[1,2] Especially, current investigations for the self-assembled lipid nanotubes have been focusing on precise dimension control,[3−5] their alignment on a solid substrate,[6−10] and rational functionalization of their surfaces.[3,11−14] Hydrophilic 10−100 nm scaled hollow cylinders of the lipid nanotubes can provide suitable nanospace for biomacromolecules at least 10 times larger in dimension as compared to the molecules used for conventional host−guest chemistry.[15,16] Therefore, they function as containers for nanoscale reaction,[17−19] channels for nanoscale separation,[20,21] and should act as carriers for drug delivery.[22−24] Martin et al.[25] and other authors[26,27] have

* To whom correspondence should be addressed. Fax: 81-29-861-4545. E-mail: tshmz-shimizu@aist.go.jp (T.S.).
† SORST, Japan Science and Technology Agency.
‡ National Institute of Advanced Industrial Science and Technology.
§ CREST, Japan Science and Technology Agency.
|| Nara Institute of Science and Technology.

(1) Recent reviews: (a) Shimizu, T.; Masuda, M.; Minamikawa, H. *Chem. Rev.* **2005**, *105*, 1401−1443. (b) Gao, X.; Matsui, H. *Adv. Mater.* **2005**, *17*, 2037−2050. (c) Karlsson, M.; Davidson, M.; Karlsson, R.; Karlsson, A.; Bergenholtz, J.; Konkoli, Z.; Jesorka, A.; Lobovkina, T.; Hurtig, J.; Voinova, M.; Orwar, O. *Annu. Rev. Phys. Chem.* **2004**, *55*, 613−649. (d) Martin, C. R.; Kohli, P. *Nat. Rev. Drug Discovery* **2003**, *2*, 29−37.
(2) Recent issues: (a) Carny, O.; Shalev, D. E.; Gazit, E. *Nano Lett.* **2006**, *6*, 1594−1597. (b) Yamamoto, Y.; Fukushima, T.; Suna, Y.; Ishii, N.; Saeki, A.; Seki, S.; Tagawa, S.; Taniguchi, M.; Kawai, T.; Aida, T. *Science* **2006**, *314*, 1761−1764. (c) Ashkenasy, N.; Horne, W. S.; Ghadiri, M. R. *Small* **2006**, *2*, 99−102. (d) Raviv, U.; Needleman, D. J.; Li, Y.; Miller, H. P.; Wilson, L.; Safinya, C. R. *Proc. Natl. Acad. Sci. U.S.A.* **2005**, *102*, 11167−11172. (e) Litvinchuk, S.; Sorde, N.; Matile, S. *J. Am. Chem. Soc.* **2005**, *127*, 9316−9317. (f) Nomura, S. M.; Mizutani, Y.; Kurita, K.; Watanabe, A.; Akiyoshi, K. *BBA Biomembrane* **2005**, *1669*, 164−169. (g) Lee, S. B.; Koepsel, R.; Stolz, D. B.; Warriner, H. E.; Russell, A. J. *J. Am. Chem. Soc.* **2004**, *126*, 13400−13405. (h) John, G.; Mason, M.; Ajayan, P. M.; Dordick, J. S. *J. Am. Chem. Soc.* **2004**, *126*, 15012−15013.
(3) Masuda, M.; Shimizu, T. *Langmuir* **2004**, *20*, 5969−5977.
(4) Kamiya, S.; Minamikawa, H.; Jun, J. H.; Yang, B.; Masuda, M.; Shimizu, T. *Langmuir* **2005**, *21*, 743−750.
(5) Singh, A.; Wong, E. M.; Schnur, J. M. *Langmuir* **2003**, *19*, 1888−1898.
(6) Karlsson, A.; Karlsson, R.; Karlsson, M.; Cans, A.-S.; Stromberg, A.; Ryttsen, F.; Orwar, O. *Nature* **2001**, *409*, 150−152.
(7) Frusawa, H.; Fukagawa, A.; Ikeda, Y.; Araki, J.; Ito, K.; John, G.; Shimizu, T. *Angew. Chem., Int. Ed.* **2003**, *42*, 72−74.
(8) Mahajan, N.; Fang, J. *Langmuir* **2005**, *21*, 3153−3157.
(9) Brazhnik, K. P.; Vreeland, W. N.; Hutchison, J. B.; Kishore, R.; Wells, J.; Helmerson, K.; Locascio, L. E. *Langmuir* **2005**, *21*, 10814−10817.
(10) Guo, Y.; Yui, H.; Fukagawa, A.; Kamiya, S.; Masuda, M.; Ito, K.; Shimizu, T. *J. Nanosci. Nanotechnol.* **2006**, *6*, 1464−1466.
(11) Kameta, N.; Masuda, M.; Minamikawa, H.; Goutev, N. V.; Rim, J. A.; Jung, J. H.; Shimizu, T. *Adv. Mater.* **2005**, *17*, 2732−2736.
(12) Fuhrhop, J.-H.; Tank, H. *Chem. Phys. Lipids* **1987**, *43*, 193−213.
(13) Fuhrhop, J.-H.; Spiroski, D.; Boettcher, C. *J. Am. Chem. Soc.* **1993**, *115*, 1600−1601.
(14) Claussen, R. C.; Rabatic, B. M.; Stupp, S. I. *J. Am. Chem. Soc.* **2003**, *125*, 12680−12681.
(15) MacGilivray, L. R.; Atwood, J. L. In *Advances in Supramolecular Chemistry*; Gokel, G. W., Ed.; JAI Press: Stamford, CT, 2000; Vol. 6, pp 157−183.
(16) Biradha, K.; Fujita, M. In *Advances in Supramolecular Chemistry*; Gokel, G. W., Ed.; JAI Press: Stanford, CT, 2000; Vol. 6, pp 1−39.
(17) Yang, B.; Kamiya, S.; Yoshida, K.; Shimizu, T. *Chem. Commun.* **2004**, 500−501.
(18) Yang, B.; Kamiya, S.; Shimizu, Y.; Koshizaki, N.; Shimizu, T. *Chem. Mater.* **2004**, *16*, 2826−2831.
(19) Yui, H.; Guo, Y.; Koyama, K.; Sawada, T.; John, G.; Yang, B.; Masuda, M.; Shimizu, T. *Langmuir* **2005**, *21*, 721−727.
(20) Shimizu, T. *J. Polym. Sci., Part A* **2006**, *44*, 5137−5152.
(21) Sott, K.; Lobovkina, T.; Lizana, L.; Tokarz, M.; Bauer, B.; Konkoli, Z.; Orwar, O. *Nano Lett.* **2006**, *6*, 209−214.
(22) Schnur, J. M.; Price, R.; Rudolph, A. S. *J. Controlled Release* **1994**, *28*, 3−13.

10.1021/cm070626p CCC: $37.00 
Published on Web 06/09/2007

**Scheme 1**

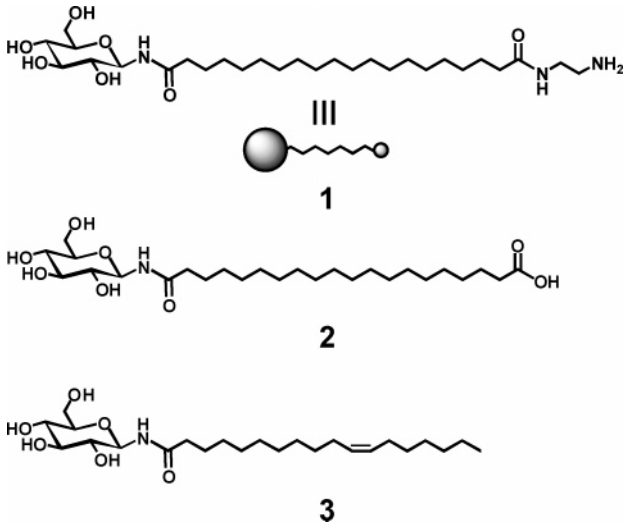


developed $SiO_2$-nanotubes with functionalized inner surfaces, which can encapsulate drugs, proteins, DNAs, and hydrophobic dyes via electrostatic and hydrophobic interactions. The self-assembled lipid nanotubes should be not less useful than such template-assisted nanotubes in terms of their characteristics including mild self-assembly process, thermoreversible formation and deformation, tunable inner and outer surfaces, controllable inner diameters (10−100 nm), and high biodegradability and compatibility.[1a]

Heteroditopic 1,$\omega$-bipolar amphiphiles are known as unsymmetrical bolaamphiphiles in which two hydrophilic headgroups of different sizes and properties are connected to a hydrophobic spacer at each end. Their unsymmetry should allow them to become candidates for the self-assembly into nanotubes having different inner and outer surfaces.[28] We have recently found that the self-assembly of a series of unsymmetrical bolaamphiphiles, *N*-(2-aminoethyl)-*N*′-($\beta$-D-glucopyranosyl)-alkanediamide (Scheme 1), in alkaline aqueous solutions can selectively give nanotubes by optimizing the initial molecular packing and the length of the oligomethylene spacer of the bolaamphiphiles.[11,29] The obtained nanotubes (abbreviated as "W-nanotubes" hereafter, 80 nm inner diameter) were found to have different inner and outer surfaces covered with amino- and glucose headgroups, respectively, and to encapsulate negatively charged nanoparticles and ferritin (spherical proteins) into the hollow cylinder. Here, we demonstrate for the first time the modification of the inner surface with a fluorescent molecule as an optical sensing moiety to visualize the dynamic encapsulation and nanofluidic features of ferritin and DNA in the hollow channel of the resultant W-nanotube. We also discuss the size and surface charge effects of the nanotube hollow channel on the effective encapsulation of the biomacromolecules.

## Results and Discussion

**Functionalization of the Nanotube Inner Surfaces.** Chemical modification was carried out to visualize the encapsulation and nanofluidic behavior of a guest spherical protein in the nanotube channels by fluorescence resonance energy transfer (FRET) technique. We employed 4-fluoro-7-nitrobenzofurazan (NBD-F) as a fluorescence donor dye to covalently modify the amino groups on the inner surfaces of the W-nanotube. NBD-F strongly fluoresces only when reacted with the amino group, although NBD-F itself has no fluorescence.[30] The surface modification was performed as follows: The acetonitrile solution of NBD-F (18 mM, 1 mL) was added into the aqueous dispersion of the W-nanotube (1 mg/mL, [**1**] = 2.0 mM, 9 mL) at pH 8 adjusted by borate buffer. The mixed solution was stirred at 60 °C for 1 min and then cooled to room temperature. Unreacted NBD-F was removed through a polycarbonate membrane filter with 0.2 $\mu$m pore size. Most of the W-nanotubes were collected over the membrane because of their high-axial-ratio nanostructures. UV−vis absorption spectrum of the separated NBD-F indicated that about 10% of initial NBD-F in mole ratio participate in the reaction with the amino groups. We observed neither morphological changes nor destruction of the W-nanotubes after the chemical modification (see the Supporting Information). Fluorescence optical microscopy (Figure 1a) clearly visualized the NBD-immobilized W-nanotube (abbreviated as NBD-nanotube hereafter), proving that NBD is covalently linked to the inner surfaces of the W-nanotube. A quenching experiment using the FRET system as shown later can also support the presence of NBD at the inner surface.

**Dynamic Encapsulation Behavior.** UV−vis, fluorescence spectroscopy, and time-lapse fluorescence microscopy were useful in examining the dynamic behavior of encapsulation and transportation of 1−10 nm scale objects in the NBD-nanotube channels. We chose ferritin[31] as a guest protein, because the Fe atoms in the ferrihydrite core of the spherical proteins efficiently shield the electron beam and give a high-contrast TEM image without staining. Ferritin was labeled with the fluorescence acceptor dye, QSY7, which can efficiently quench NBD by the FRET mechanism. Dynamic light scattering and $\zeta$-potential measurements showed that the QSY7-labeled ferritin (abbreviated as QSY7-ferritin hereafter) is 14.7 nm wide and negatively charged (−29.9 to −35.4 mV) at pH 6.5−9 (see the Supporting Information).

(23) Spargo, B. J.; Cliff, R. O.; Rollwagen, F. M.; Rudolph, A. S. *J. Microencapsulation* **1995**, *12*, 247−254.
(24) Meilander, N. J.; Pasumarthy, M. K.; Kowalczyk, T. H.; Cooper, M. J.; Bellamkonda, R. V. *J. Controlled Release* **2003**, *88*, 321−331.
(25) Selected issues: (a) Mitchell, D. T.; Lee, S. B.; Trofin, L.; Li, L.; Nevanen, T. K.; Soederlund, H.; Martin, C. R. *J. Am. Chem. Soc.* **2002**, *124*, 11864−11865. (b) Lee, S. B.; Mitchell, D. T.; Trofin, L.; Nevanen, T. K.; Soederlund, H.; Martin, C. R. *Science* **2002**, *296*, 2198−2200. (c) Kohli, P.; Martin, C. R. *Drug News Perspect.* **2003**, *16*, 566−573.
(26) (a) Son, S. J.; Lee, S. B. *J. Am. Chem. Soc.* **2006**, *128*, 15974−15975. (b) Son, S. J.; Reichel, J.; He, B.; Schuchman, M.; Lee, S. B. *J. Am. Chem. Soc.* **2005**, *127*, 7316−7317. (c) Jayaraman, K.; Okamoto, K.; Son, S. J.; Luckett, C.; Gopalani, A. H.; Lee, S. B.; English, D. S. *J. Am. Chem. Soc.* **2005**, *127*, 17385−17392.
(27) Chen, C.-C.; Liu, Y.-C.; Wu, C.-H.; Yeh, C.-C.; Su, M.-T.; Wu, Y.-C. *Adv. Mater.* **2005**, *17*, 404−407.
(28) Fuhrhop, J.-H.; Wang, T. *Chem. Rev.* **2004**, *104*, 2901−2938.
(29) Kameta, N.; Masuda, M.; Minamikawa, H.; Shimizu, T. *Langmuir* **2007**, *23*, 4634−4641.
(30) Miyano, H.; Toyooka, T.; Imai, K. *Anal. Chem. Acta* **1985**, *170*, 81−87.
(31) (a) Proulx-Curry, P. M.; Chasteen, N. D. *Coord. Chem. Rev.* **1995**, *144*, 347−368. (b) Silk, S. T.; Breslow, E. *J. Biol. Chem.* **1976**, *251*, 6963−6973.

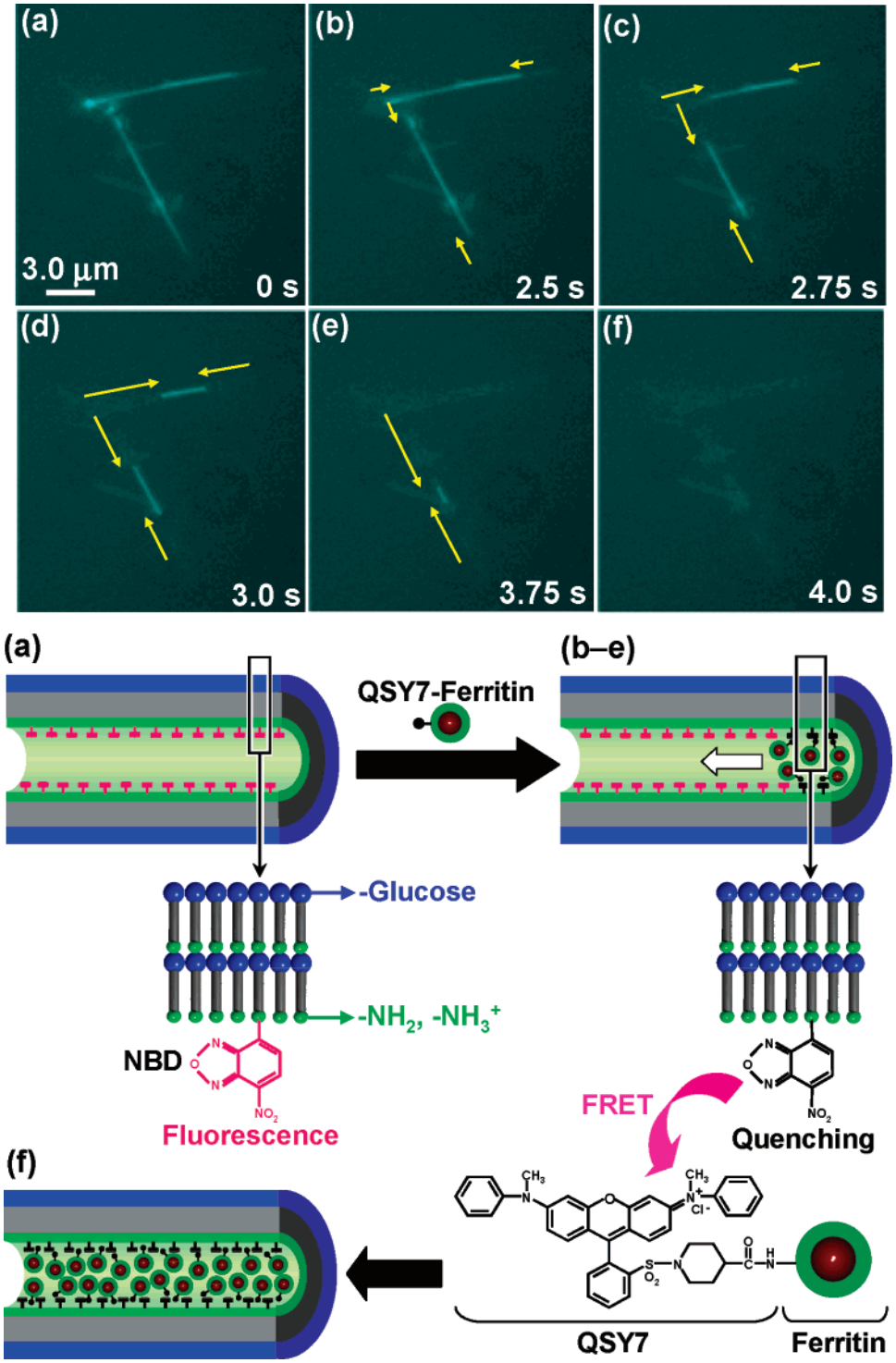


**Figure 1.** Time-lapse fluorescence microscopic images of the NBD nanotubes upon addition of QSY7-ferritin. The time course was indicated in the bottom right of each figure.

Figure 2 shows the fluorescence spectra of the NBD-nanotubes in the absence and presence of the QSY7-ferritin. In this system, the FRET system takes place only when the NBD-nanotube is encapsulating and approaching the QSY7-ferritin in the nanochannel. The lipid membrane wall of the W-nanotubes is thick enough (15 nm)[29] to prevent FRET through the wall from the internal NBD to the external QSY7-ferritin existing in a bulk solution. Indeed, the fluorescence band of the NBD-nanotube disappeared at neutral pH (pH 6.8) in the presence of the QSY7-ferritin. This finding is ascribable to quenching phenomenon based on FRET from the internal NBD to the QSY7-ferritin encapsulated in the hollow cylinder of the NBD-nanotube. TEM observation obviously evidenced the encapsulation of the QSY7-ferritin into the NBD-nanotube (see the Supporting Information). The following three control experiments can also support the quenching by FRET: (1) no quenching of the NBD-nanotube upon addition of intact ferritin, (2) rapid quenching upon addition of QSY7 itself as discussed later, and (3) no remarkable quenching phenomena under alkaline conditions (pH 9 in Figure 2). Electrostatic interaction between positively charged inner surfaces at pH 6.8 and

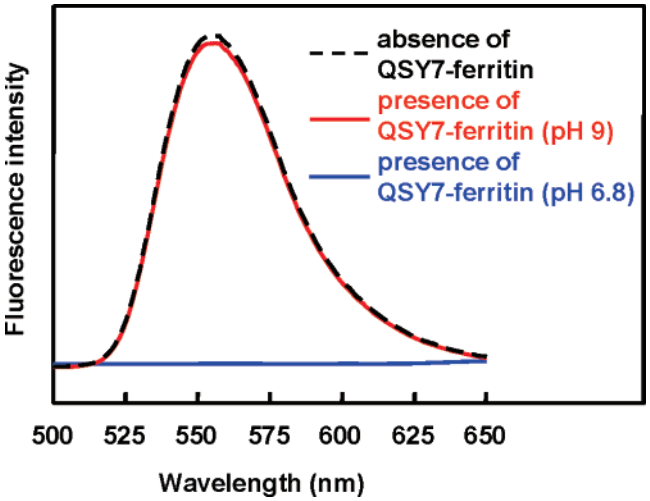


**Figure 2.** Fluorescence spectra of the NBD nanotube in the presence of QSY7-ferritin (solid lines) and in the absence of QSY7-ferritin (dotted line) in aqueous solutions at pH 6.8 and 9. Excitation at 470 nm.

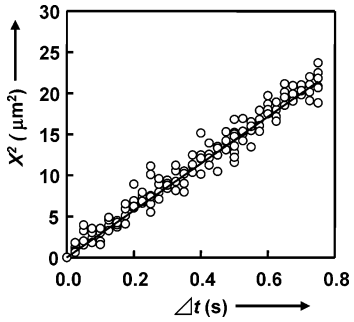


**Figure 3.** Relationship between the square of the migration distance ($X^2$) of the QSY7-ferritin in the lipid nanotube channels and the time ($\Delta t$) required for migration.

negatively charged QSY7-ferritin should also be effective for encapsulation as described in later. Alkaline conditions suppress the encapsulation ability of the nanotube because of deprotonation of the ammonium groups on the inner surfaces and the resultant less electrostatic interaction with QSY7-ferritin.

Fluorescence microscopic observation revealed that upon addition of the QSY7-ferritin, both open ends of the NBD-nanotubes start to quench (Figure 1b) and the quenching gradually moves toward the central part with lapse of time (Figure 1c−e). The quenching completes in a few seconds (Figure 1f). The following view details the experimental finding. The QSY7-ferritin as a quencher penetrates into the NBD-nanotube from the outside and gradually quenches the entire NBD dyes of the inner surfaces with flowing inside the nanochannels shaped by the hollow cylinder. This time-dependent quenching behavior also proves that the nanochannel shaped by the hollow cylinder structure is completely isolated from the external solution and exposed to the aqueous environment only at both ends.

**Nanofluidic Behavior of Ferritin in the Nanochannels.** The analysis for the obtained several time-lapse images demonstrated that a diffusion phenomenon can well-simulate this nanofluidic feature of the QSY7-ferritin. The square of migration distance ($X^2$) of the QSY7-ferritin was plotted against the time laps ($\Delta t$) required for migration (Figure 3). The obtained linear plot is clearly compatible with the diffusion process. In the present system, the QSY7-ferritin exists richly in the external solution and then diffuses from the open ends of the nanotube ($X = 0$) to the central part of the hollow cylinder ($X > 0$). Therefore, we can apply the equation $[X^2] = 4D\Delta t$ to this system, where $D$ is a diffusion constant.[32] On the basis of the slope for the linear relationship, we evaluated the diffusion constant $D$ of the QSY7-ferritin in the NBD-nanotube channel as $0.7 \times 10^{-11}$ m$^2$ s$^{-1}$. The $D$ value is 5 times smaller than that of the QSY7-ferritin in a bulk aqueous solution ($D = 3.4 \times 10^{-11}$ m$^2$ s$^{-1}$, independently evaluated on the basis of dynamic light scattering experiment and Einstein−Stokes equation, see the Supporting Information). We can envisage several possible causes for the relatively smaller $D$ value. The electrostatic interactions between the positively charged inner surfaces and the negatively charged guest QSY7-ferritin would allow the diffusion to slow. Relatively larger viscosity of the water in the nanochannel could be relevant to the smaller $D$ value, because $D$ is inversely proportional to viscosity. We have already demonstrated that the confined water in the hollow cylinder of the nanotube, having the identical inner and outer surfaces covered with glucose headgroups, possesses relatively lower polarity and higher viscosity as compared with bulk water.[19] Moreover, we could point out other possibilities such as diffusion in a restricted geometry of narrow cylinders,[33] nanopillars,[34] or diffusion associated with adsorption.[35]

Orwar et al. addressed the diffusion and velocity for the transport of fluorescent nanoparticles (30 nm) in a fluid-state lipid nanotube made from phospholipids, which connect two vesicle containers (closed system).[36] They suggested that the diffusion constant of the fluorescence particle in the nanotube of ∼200 nm inner diameters was similar to the theoretical diffusion constant for a 30 nm particle at 298 K in a 100 nm diameter tube ($D = 0.9 \times 10^{-11}$ m$^2$ s$^{-1}$).[37] This $D$ value is well-compatible with our experimental evaluation for the open nanochannel system with a solid-state lipid nanotube, which is directly exposed to bulk solution. Similarly, we have also evaluated the nanofluidic feature of a relatively smaller guest, QSY7-labeled gold nanoparticles 1.4 nm wide (abbreviated as QSY7-nanogold hereafter) and intrinsic QSY7 itself. The $D$ value for the QSY7-nanogold was calculated to be $6.2 \times 10^{-11}$ m$^2$ s$^{-1}$, which is 9 times larger than that of the QSY7-ferritin (see the Supporting Information). We were unable to determine the $D$ value of QSY7 itself under given the experimental conditions, because the diffusion of QSY7 itself was much faster than those of the QSY7-ferritin and the QSY7-nanogold. These results indicated that the size of the guest substance is one of the critical factors that determine the diffusion and the nanof-

(32) Barrow, G. M. *Physical Chemistry*, 5th ed.; McGraw-Hill: New York, 1988.
(33) Deen, V. M. *AIChE J.* **1987**, *33*, 1409−1425.
(34) Kaji, N.; Ogawa, R.; Oki, A.; Horiike, Y.; Tokeshi, M.; Baba, Y.; *Anal. Bioanal. Chem.* **2006**, *386*, 759−764.
(35) Crank, J. *The Mathematics of Diffusion*, 2nd ed.; Oxford University Press: Oxford, UK, 1980.
(36) Karlsson, R.; Karlsson, M.; Karlsson, A.; Cans, A.-S.; Bergenholtz, J.; Akerman, B.; Ewing, A. G.; Voinova, M.; Orwar, O. *Langmuir* **2002**, *18*, 4186−4190.
(37) Brenner, H.; Gaydos, L. J. *J. Colloid Interface Sci.* **1977**, *58*, 312−356.

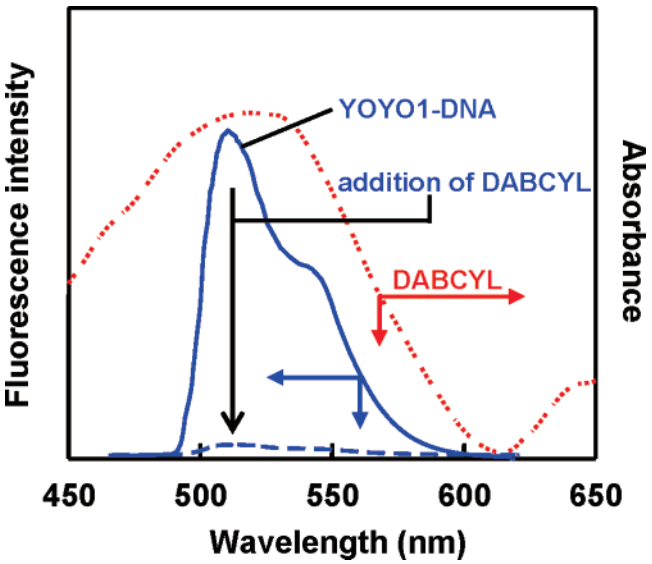


**Figure 4.** Fluorescence spectrum of the YOYO1-DNA in the presence of W-nanotube (solid line) and quenching of the fluorescence upon addition of DABCYL (dashed line). Excitation at 491 nm. Absorption spectrum of DABCYL in aqueous solutions (dotted line).

luidic features in the nanochannel. They also satisfy the general tendency in diffusion phenomena: Relatively smaller particles travel faster than relatively larger ones in the nanochannels.

**Size Effect of Inner Diameters on the Encapsulation of DNA.** We are also able to obtain the nanotubes with a 20 nm inner diameter (abbreviated as the "N-nanotubes" hereafter) by self-assembly of **1** in water at pH 6 (see Experimental Section). The molecular packing analysis by X-ray diffraction and IR measurements revealed that in manner similar to that of the W-nanotubes,[11,29] the N-nanotubes have different inner and outer surfaces covered with the amino and glucose headgroups, respectively (see Experimental Section and the Supporting Information). Therefore, we compared the encapsulation ability of the two nanotubes with different inner diameters toward a double strand DNA.

T4GT7-DNA, characterized by 166 kbp and 56 $\mu$m extended length and labeled with the fluorescence dye YOYO-1 (abbreviated as YOYO1-DNA hereafter), was mixed with the aqueous solutions containing the W-nanotubes with 80 nm inner diameter at pH 7.5. YOYO-1 itself is nonfluorescent in the solution, but forms highly fluorescent complexes with the double strand DNA (Figure 4).[38] Illuminating the YOYO1-DNA gave two different types of fluorescence images (Figure 5b). One takes a random coil conformation located just outside of the W-nanotube, whereas the other is located straight along the one-dimensional direction of the W-nanotube (images a and b of Figure 5). These results suggested that the part of the YOYO1-DNA should be encapsulated into the hollow cylinder of the W-nanotube or adsorbed on its outer surface. To further confirm these features, we carried out time-laps fluorescence microscopic measurement combined with the FRET system. We then chose DABCYL as a fluorescence acceptor dye for the FRET system with the YOYO1-DNA as a donor, because the absorption band of DABCYL completely overlaps with the fluorescence band of the donor YOYO1-DNA (Figure 4). Therefore, the fluorescence of the YOYO1-DNA can be quenched via FRET when the dyes are close to each other (within a few nanometers). Indeed, the fluorescence from the mixture of YOYO1-DNA and the W-nanotube was completely quenched upon the addition of DABCYL (Figure 4).

Time-lapse fluorescence microscopic observation revealed that upon addition of DABCYL, quenching of the fluorescence starts from both open ends of the W-nanotubes (Figure 5c) and gradually moves toward the central part with lapse of time (Figure 5d−f). This phenomenon is compatible with the following view: DABCYL in the bulk solution penetrated into the W-nanotube from the open ends and then started to quench the YOYO1-DNA fluorescence encapsulated in the W-nanotube via FRET. Within a few seconds, DABCYL diffused to reach the middle of the W-nanotube and completed the quenching of the whole nanotube. The fluorescence image from the YOYO1-DNA located just outside was found to be quenched much faster (within 0.3 s, images b and c of Figure 5) than that of the encapsulated one (~1.0 s, Figure 5b−f). Therefore, it is distinguishable as the YOYO1-DNA locating outside of the W-nanotube. All results demonstrated that the W-nanotube can encapsulate long T4GT7-DNA into the hollow cylinder as well as ferritin.

On the other hand, the N-nanotube showed no encapsulation ability toward the YOYO1-DNA, although the inner diameter (~20 nm) is large enough to accommodate the DNA (2 nm width). The observed difference in the DNA encapsulation behavior between the W- and N-nanotubes can be explained by the persistance length of the double-strand DNA, typically 50 nm.[39] The entrance of the W-nanotube (~80 nm inner diameter) is wide enough to accommodate the persistance region of the DNA chain via electrostatic interaction. This circumstance can allow the long T4GT7-DNA to migrate into the middle of the W-nanotube by dynamic deformation and is also well compatible with the view that the N-nanotubes having 20 nm inner diameters cannot encapsulate the DNA effectively.

**Surface Charge Effect on the Encapsulation of Spherical Proteins.** To elucidate the effect of the electrostatic interaction on the encapsulation, we investigated the encapsulation ability of the nanotubes with different inner surfaces toward spherical proteins. As a cationic guest protein, we selected starvation-induced DNA-binding protein (Dps) with a ferrihydrite core, as well as ferritin. Dps consisting of 12 subunits (9 nm wide) can bind anionic groups, such as phosphoric acid in DNA.[40] Although the net charge of Dps is negative at neutral pH (pI = 4.7), it has a partly positive

(38) (a) Rye, H. S.; Yue, Stephen.; Wemmer, D. E.; Quesada, M. A.; Haugland, R. P.; Mathies, R. A.; Glazer, A. N. *Nucleic Acids Res.* **1992**, *20*, 2803−2812. (b) Netzel, T. L.; Nafisi, K.; Zhao, M.; Lenhard, J. R.; Johnson, I. *J. Phys. Chem.* **1995**, *99*, 17936−17947.

(39) Wang, M. D.; Yin, H.; Landick, R.; Gelles, J.; Block, S. M. *Biophys. J.* **1997**, *72*, 1335−1346.

(40) Frenkiel-Krispin, D.; Ben-Avraham, I.; Englander, J.; Shimoni, E.; Wolf, S. G.; Minsky, A. *Mol. Microbiol.* **2003**, *51*, 395−405.

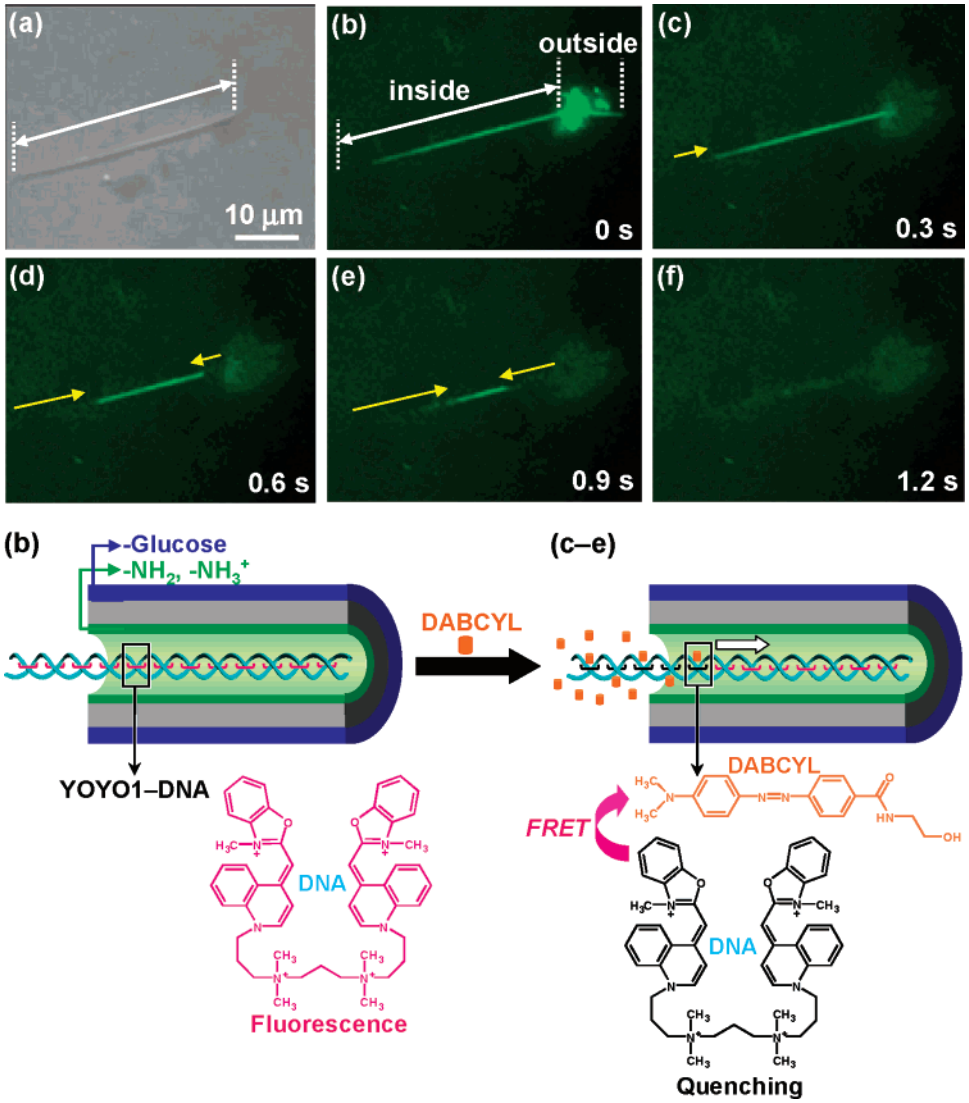


**Figure 5.** (a) Optical microscopic (phase contrast) image and (b−f) time-lapse fluorescence microscopic images of the YOYO1-DNA encapsulated in the W-nanotube upon addition of DABCYL. The time course was indicated in the bottom right of each figure.

charged domain on the surface.[41] TEM images revealed that the W- and N-nanotubes never encapsulated the partly positively charged Dps at pH 6.8 after mixing the solutions containing the nanotubes and proteins (images b and d in Figure 6), although both nanotubes can effectively encapsulate the negatively charged ferritin into their hollow cylinders (images a and c in Figure 6). These results suggest that the positively charged inner surfaces of the nanotubes strongly accelerate the encapsulation of the negatively charged ferritin via electrostatic interaction. To confirm the contribution of the electrostatic interaction to the encapsulation, we also examined the encapsulation ability of the self-assembled lipid nanotubes from **2**[3] and **3**[4] with different surface characteristics. The former nanotubes have approximately 20 nm inner diameters, giving distinct inner and outer surfaces covered with negatively charged carboxylate and nonionic glucose headgroups, respectively. The latter have approximately 60 nm inner diameters, providing identical inner and outer surfaces covered with nonionic glucose headgroups. The latter nonionic nanotubes of **3** showed no encapsulation ability (see the Supporting Information), although the lyophilized nanotubes of **3** were able to encapsulate ferritin via capillary force reported previously.[42] The former carboxylate nanotubes of **2** displayed behavior opposite that of the N- and W-nanotubes. Namely, the self-assembled nanotubes from **2** were able to effectively encapsulate the partly positively charged Dps into their hollow cylinders (Figure 6e), whereas they never encapsulated the negatively charged ferritin (Figure 6f).

The lipid nanotubes with unsymmetrical inner and outer surfaces, thus, have intriguing advantages to be easily and selectively functionalized under mild conditions. This feature is in contrast with that of biological nanopores,[43−45] carbon,[46−48]

(41) (a) Almiron, M.; Link, A. J.; Furlong, D.; Kolter, R. *Genes Dev.* **1992**, *6*, 2646−2654. (b) Grant, R. A.; Filman, D. J.; Finkel, S. E.; Kolter, R.; Hogle, J. M. *Nat. Struct. Biol.* **1998**, *5*, 294−303. (c) Ilari, A.; Ceci, P.; Ferrari, D.; Rossi, G. L.; Chiancone, E. *J. Biol. Chem.* **2002**, *277*, 37619−37623.

(42) Yui, H.; Shimizu, Y.; Kamiya, S.; Yamashita, I.; Masuda, M.; Ito, K.; Shimizu, T. *Chem. Lett.* **2005**, *34*, 232−233.
(43) Deamer, D. W.; Branton, D. *Acc. Chem. Res.* **2002**, *35*, 817−825.
(44) Bayley, H.; Cremer, P. S. *Nature* **2001**, *413*, 226−230.
(45) Bayley, H.; Martin, C. R. *Chem. Rev.* **2000**, *100*, 2575−2594.
(46) Ito, T.; Sun, L.; Crooks, R. M. *Chem. Commun.* **2003**, 1482−1483.
(47) Yanagi, K.; Miyata, Y.; Kataura, H. *Adv. Mater.* **2006**, *18*, 437−441.
(48) Cui, D.; Ozkan, C. S.; Ravindran, S.; Kong, Y.; Gao, H. *MCB* **2004**, *1*, 113−121.

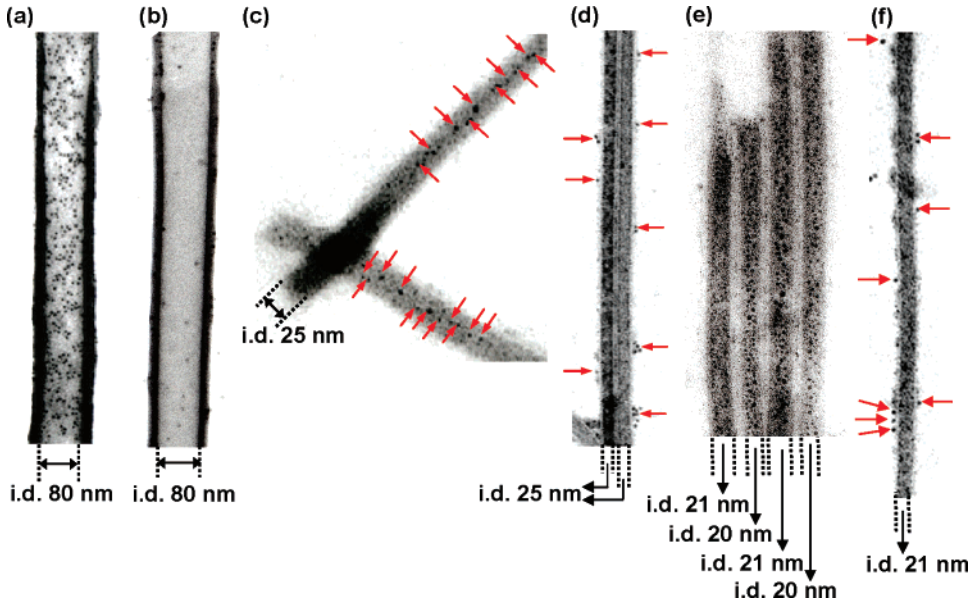


**Figure 6.** TEM images for the nanotubes showing encapsulation and no encapsulation abilities for ferritin and Dps. (a) The W-nanotube encapsulating ferritin in the hollow cylinder, (b) the W-nanotube showing no encapsulation ability for Dps, (c) the N-nanotubes encapsulating ferritin in the hollow cylinder, and (d) the N-nanotubes showing no encapsulation ability for Dps. Dps locates only outside of the nanotubes. (e) Carboxylate-nanotube self-assembled from **2**, encapsulating Dps in the hollow cylinder, and (f) the carboxylate-nanotube self-assembled from **2**, showing no encapsulation ability for ferritin. Ferritin locates only outside of the nanotube.

inorganic,[49] silica,[25−27] and polymer nanotubes[50,51] as artificial nanochannels. We are also able to deposit such lipid nanotubes to align on a solid substrate by a microextrusion method.[7,10] Therefore, the mesoscale host−guest chemistry performed by the lipid nanotube is applicable for constructing biosensing, nanototal analysis system (nanoTAS), targeting drug delivery, and medical diagnosis systems.

## Conclusion

We have for the first time succeeded in the selective covalent linking of a fluorescence-donor dye to the amino groups on the inner surfaces of the lipid nanotubes. Time-lapse fluorescence microscopy combined with the FRET system enabled us to visualize dynamic encapsulation and nanofluidic behavior of the spherical protein ferritin, gold nanoparticles, and a label reagent in the nanochannels shaped by the nanotube hollow cylinders. We have also demonstrated that the size and surface charge of the nanochannel strongly influence the effective encapsulation of the biomacromolecules such as spherical proteins and a double-stranded DNA.

## Experimental Section

**Preparation of N-Nanotube.** Prior to self-assembly in water, the synthetic compound **1** as a powder state was changed to a film state by dissolving it in *N*,*N*-dimethylformamide (DMF) and evaporating the solvent at 80 °C in vacuo.[11] The film was dispersed in water adjusted to pH 6 with HCl under reflux conditions, and the obtained hot aqueous solutions were allowed to gradually cool to room temperature. After the solution was aged for several weeks, the N-nanotubes were obtained through morphological transformation from the first formed helical coils. Atomic force microscopy, laser scan microscopy, and TEM observations revealed that most of the helical coils are converted into the N-nanotubes with 20 nm in inner diameters and 6 nm in thickness (see the Supporting Information). Some N-nanotubes exhibited a helical structure around the terminal and helical marks on the outer surface.

**Packing Analysis of N-Nanotube**. (All data are shown in the Supporting Information.) Powder X-ray diffraction (XRD) and IR measurements were performed for the lyophilized N-nanotube as well as the W-nanotube.[11] XRD measurement gave a diffraction peak in the small-angle region, indicating that N-nanotubes consist of monolayer lipid membranes (MLMs) with a stacking periodicity (*d*). By comparing the *d* value and extended molecular length (*L*), the MLM type ("polymorph") of the self-assemblies from bolaamphiphiles is predictable.[3,11,29] For unsymmetrical MLMs with an $\alpha/\beta$ interface ($\alpha$ denotes relatively larger headgroup of the unsymmetrical bolaamphiphile and $\beta$ the relatively smaller headgroup), the *d* value is much smaller or slightly smaller than *L* depending on the molecular tilt angle. The *d* values of the N-nanotube (2.87 nm) are obviously shorter than the *L* (3.78 nm). Therefore, the N-nanotubes should consist of unsymmetrical MLMs with an $\alpha/\beta$ interface with large molecular tilt (41°). The $\delta(CH_2)$ scissoring band in the IR spectrum reflect the subcell structure of the oligomethylene spacer of self-assembly. A single sharp peak of the $\delta(CH_2)$ band for the N-nanotubes with full width at half-maximum of less than 10 $cm^{-1}$ strongly suggests a triclinic parallel ($T_{//}$) or monoclinic parallel ($M_{//}$) subcell type. This result clarified that molecules packed in parallel fashion within the MLMs.[29]

**Preparation of QSY7-Ferritin.** QSY7-ferritin was prepared on the basis of known protocols.[52] A methanol solution of QSY7carboxylic acid succinimidyl ester (Molecular Probes, 70 mM, 10 $\mu$L) was added to 1 mL of equine spleen ferritin solution (CALBIOCHEM; 10 mM, 5 mg/mL, MW = 500 000) at pH 8.5 adjusted by HEPES buffer. The both concentrations were defined by considering the number of amino groups in lysine residues located on the

(49) Goldberger, J.; Fan, R.; Yang, P. *Acc. Chem. Res.* **2006**, *39*, 239−248.
(50) Tian, Y.; He, Q.; Tao, C.; Li, J. *Langmuir* **2006**, *22*, 360−362.
(51) Abidian, M. R.; Kim, D.-H.; Martin, D. C. *Adv. Mater.* **2006**, *18*, 405−409.
(52) Li, M.; Wong, K. K. W.; Mann, S. *Chem. Mater.* **1999**, *11*, 23−26.

external surface of ferritin. Namely, the concentration of the used QSY7 was about 70 times as large as that of ferritin since ferritin has 60−70 lysine residues on the external surface. The mixed solution was stirred for 12 h at r.t. and then was centrifuged (by amicon centriprep, MILLIPORE) to remove low-molecular-weight molecules such as unreacted QSY7 and succinimidyl moiety. The amount of reacted QSY7 was estimated to be 20% of the initially used QSY7 by UV−vis absorption spectroscopy. Particle size and $\zeta$-potential of the QSY7-ferritin were measured by dynamic light scattering, indicating that it has 14.7 nm diameter and negatively charged surface under neutral pH conditions. This finding is reasonable when considering 12 nm diameter[31a] and the isoelectric point (pI = 4.6)[31b] of intact ferritin. TEM observation revealed that the obtained QSY7-ferritin shows no aggregation during encapsulation experiments.

**Preparation of Dps.** The plasmid expression vector for Dps was constructed by cloning of the *E. coli* dps gene and its fragments into pET3a between the *NdeI* and *HindIII* sites. The *E. coli dps* gene was amplified by PCR using oligonucleotide primers containing the point base substitutions to generate cloning sites at the ends of fragments. The cloned PCR product was confirmed by DNA sequencing. *E. coli* cells harboring the recombinant plasmid constructed as described above were grown at 30 °C in Luria−Bertani (LB) broth containing 50 mg/mL ampicillin until the culture reached an optical density of 0.5 at 600 nm, and then isopropyl-1-thio-$\beta$-D-galactopyranoside (IPTG) was added to a final concentration of 0.5 mM. After cultivation for 12 h at 16 °C, the cells were harvested by centrifugation and washed with 25 mM potassium phosphate buffer, pH 7.0, and then resuspended in the same buffer. The cells were disrupted by using a sonicator (Branson Sonifier), and the resulting supernatant was applied to a HiTrap Heparin HP column (Amersham Bioscience). After the column was washed with 50 mM Tris-HCl buffer (pH 7.0), Dps was eluted with a 0−1 M NaCl gradient. Final purification of the Dps was performed by using a Superdex-30 size excursion column; it was then dialyzed against 50 mM HEPES (pH 7.0) containing 0.5 M NaCl. Iron-loaded Dps was prepared by incubation of 5 $\mu$m apo-Dps with 50 mM ferrous ammonium sulfate overnight, followed by purification through gel-filtration on Superdex-30 size exclusion column.

**Encapsulation Experiment.** An aqueous dispersions of spherical proteins such as ferritin (CALBIOCHEM, cadmium-free, from Equine Spleen) or Dps were centrifuged (by amicon cetriprep, MILLIPORE) to remove buffers and salts contained in advance. Ferritin or Dps free from buffers and salts was added to the aqueous dispersion containing the corresponding nanotube (1 mg/mL) at pH 6.8 adjusted by HCl and NaOH. The concentration of the proteins was adjusted to 5 mg/mL. After being aged overnight, the solution was filtered by using polycarbonate membrane with a 0.2 $\mu$m pore size. The residual nanotubes were washed several times to remove the proteins existing outside of the nanotubes.

T4GT7-DNA (Nippon Gene, 166 kbp) was labeled with the bis-intercalating fluorescent dye, YOYO-1 (Molecular Probes), at a ratio of 1 dye per 5 bp. The working solution of the labeled DNA (abbreviated as YOYO1-DNA) was adjusted to a concentration of 3 $\mu$g/mL of 1×TE buffer (10 mM Tris HCl, 1 mM EDTA, pH 8.0) including 2-mercaptoethanol (2 vol %) as a radical scavenger. In a typical DNA encapsulation experiment, the DNA working solution was added to the aqueous solution of the nanotube at pH 7.5. The mixed solution was kept at 4 °C overnight and observed by fluorescence microscope without further purification.

**TEM and STEM Observations.** Aqueous dispersions of each assembly were dropped onto a carbon grid, and dried by standing at room temperature. The guest-free nanotubes, helical coils, and tapes, negatively stained with a phosphotungstate solution (2 wt %, pH adjusted to 9 by NaOH), were observed by TEM (Hitachi H-7000) and STEM (Hitachi S-4800) operated at 75 and 30 kV, respectively.

**AFM Observations.** Aqueous dispersions of nanotubes were dropped onto freshly cleaved mica and dried by standing at room temperature. AFM images were recorded under ambient conditions using a Nanosearch SFT-3500 (SHIMADZU) operating in the tapping mode regime. Microfabricated silicon cantilever tips (NCHR) with a resonance frequency of approximately 285 kHz and a spring constant of about 42 $Nm^{-1}$ were used.

**Powder XRD and IR Measurements.** The obtained nanotubes, helical coils, and tapes were lyophilized and subjected to XRD measured at 25 °C with a Rigaku diffractometer (Type 4037) using graded *d*-space elliptical side-by-side multilayer optics, monochromated Cu K$\alpha$ radiation (40 kV, 30 mA), and an imaging plate (R-Axis IV). IR spectra were measured with a Fourier transform IR spectrometer (JASCO FT-620) and an attenuated total reflection (ATR) accessory system (Diamond MIRacle, horizontal ATR accessory with a diamond crystal prism, PIKE Technologies, USA).

**Time-Lapse Fluorescence Microscopic Observation.** Fluorescence microscopic observation for the nanotube encapsulating YOYO1-DNA and NBD-nanotube was performed using an inverted microscope (OLYMPUS IX71) equipped with a CCD camera (HAMAMATSU ORCA-ER). Excitation optical source was prepared by a high-pressure mercury lump (100 W, OLYMPUS BH2-REL-T3) and a 483−501 nm band-pass filter. Time-lapse fluorescence microscopic images for the nanotube encapsulating YOYO1-DNA and NBD-nanotube upon addition of fluorescence acceptor dye DABCYL (Molecular Probe) and QSY7-ferritin, respectively, were recorded on a PC by AQUACOSMOS system (HAMAMATSU). The measurement interval was set to 50−300 ms.

**Spectrophotometric Observations.** UV−vis and fluorescence spectra of the NBD-nanotube, QSY7-ferritin, YOYO1-DNA, and DABCYL in aqueous solutions were measured at room temperature using a U-3300 spectrophotometer (HITACHI) and F-4500 spectrophotometer (HITACHI), respectively.

**Acknowledgment.** We thank Mr. Akinori Kogure at SHIMADZU Corp. for his skillful measurement for the AFM of nanotubes. We also thank Dr. Takeshi Sasaki and Dr. Shoko Kamiya at NARC, AIST, for suggestion on the DLS measurement and the preparation of glycolipid nanotubes, respectively.

**Supporting Information Available:** DLS results of QSY7-ferritin; STEM and TEM images of NBD-nanotube and NBD-nanotube encapsulating QSY7-ferritin; preparation procedure of QSY7-nanogold; investigation for the encapsulation and nanofluidic behavior of QSY7-nanogold and QSY7 in the hollow cylinder of NBD-nanotube; TEM images of the nonionic glycolipid nanotubes that showed no encapsulation ability for ferritin and Dps; confocal laser scan microscopic, AFM, and TEM images of the N-nanotubes; XRD and IR spectra of the N-nanotubes and helical coils; estimated molecular packing of the N-nanotubes and helical coils. These materials are available free of charge via the Internet at http://pubs.acs.org.

CM070626P